

LATE-TIME RADIO RE-BRIGHTENING OF GAMMA-RAY BURST AFTERGLOWS:
EVIDENCE FOR DOUBLE-SIDED JETS

Zhuo Li¹ and L.M. Song¹
Submitted to ApJL

ABSTRACT

The central engine of gamma-ray bursts (GRBs) is believed to eject double-sided ultra-relativistic jets. For an observed GRB, one of the twin jets should point toward us, and is responsible for the prompt gamma-ray and subsequent afterglow emission. We consider in this Letter the other receding jet, which will give rise to late-time radio re-brightening (RRB) when it becomes non-relativistic (NR) and radiative isotropic. The RRB peaks at a time $5t_{NR} = 2(E_{j,51}n)^{1/3}$ yr after the GRB, where t_{NR} is the observed NR timescale for the preceding jet, E_j is the jet energy and n is the ambient medium density. The peak flux is comparable to the preceding-jet emission at t_{NR} . We expect the RRB of GRB 030329 1.7 yr after the burst with a flux 0.6 mJy at 15 GHz. The cases of GRBs 970508 and 980703 have also been discussed. The detection of RRB, which needs dense monitoring campaign even a few years after a GRB, will be the direct evidence for the existence of double-sided jets in GRBs, and prove the black hole-disk system formation in the cores of progenitors.

Subject headings: gamma-rays: bursts | ISM: jets and outflows | radio continuum: general

1. introduction

A standard shock model of gamma-ray burst (GRB) afterglows has now been well established, in which the GRB outflow (jet) drives a relativistic expanding blast-wave that sweeps up and heats the GRB ambient medium to produce the long-term X-ray, optical and radio afterglow by synchrotron/inverse-Compton (IC) emission (see Zhang & Meszaros 2004 or Piran 2004 for recent reviews).

The remarkable supernova signature in GRB 030329 afterglow (Hörth et al. 2003) has confirmed that GRBs, at least the long-duration ones, are originated from explosions of massive stars. Their progenitors are believed to form black hole-disk systems in their cores, and produce double-sided jets, which are responsible for the GRB emission, along the spinning axis of the black hole (Meszaros 2002). For the observed hard GRB photons to escape freely, avoiding electron/positron pair formation, the outflows are required to be ultra-relativistic with Lorentz factor $\Gamma > 100$. Because of the relativistic beaming effect, the GRB emission is confined in a narrow cone, and can only be observed when the light of sight is within the cone. Interestingly, it was this beaming effect that made many authors expect the present of "orphan afterglows" (Rhoads 1997; Dalal, Griest, & Puet 2002; Granot et al. 2002; Granot & Loeb 2003) which correspond to θ -axis GRBs without gamma-rays associated, but with afterglows detected when the shocks decelerate.

The previous works, except for Granot & Loeb (2003), only discussed the emission from the preceding jet (PJ), which is pointing toward us, and neglected that from the other receding jet (RJ), since it always points away from us. However, in this Letter we discuss specially the emission from the RJ, which will emerge when the RJ becomes non-relativistic (NR) and the radiation becomes isotropic. Because of the light travel time delay, the RJ contribution will overlay above the late-time, already decayed PJ emission. In the NR phase the afterglow peak emission

has moved to radio frequencies, so the re-brightening from the RJ is only expected in late-time radio afterglows. We predict the late-time radio re-brightening (RRB) of GRB 030329 and discuss the long-term radio observations for two GRBs 970508 and 980703. The observation of RRBs will be particularly important due to its straightforward implication of the existence of double-sided jets in GRBs.

2. emission from the receding jet

Consider two collimated jets, that are ejected in opposite directions from the central engine of a GRB. For an observed GRB, the observer should be almost on the jet axis. We assume the two jets have the same characteristics, such as the half opening angle θ_j , the initial Lorentz factor Γ_0 , and the kinetic energy $E_j=2$ (or with equivalent isotropic energy $E_{iso} = 2E_j = \frac{2}{3}$). Since most afterglow jets seem to favor a uniform medium (Panaitescu & Kumar 2002), we assume a constant particle density n for both jets.

In the above assumptions we have taken the standard view of a homogeneous jet with sharp edge (Rhoads 1999). Recently, a structured jet model (Meszaros et al. 1998; Dai & Gou 2001; Rossi et al. 2002; Zhang & Meszaros 2002) was proposed, but detailed fits to afterglow data are still needed to determine whether it is consistent with current observations (Granot & Kumar 2003). Since the standard jet model have been well successful in the data fits (e.g., Panaitescu & Kumar 2002), we only discuss homogeneous jets here.

2.1. Jet dynamics

We first discuss the PJ. The PJ evolution can be divided into four phases. (1) Initially, $\theta = \theta_j$, the transverse size of the jet is larger than that of the causally connected region, therefore the jet evolves as if it was a conical section of a spherical relativistic blast wave. The PJ undergoes first a coasting phase with $\theta = \theta_0$. (2) After the jet-

¹ Particle Astrophysics Center, Institute of High Energy Physics, CAS, Beijing 100039, China

induced shock sweeps up enough medium, the jet kinetic energy is mostly transferred into the shocked medium, and the jet begins to decelerate significantly. This occurs at the deceleration radius $r_d = 3E_{\text{iso}} = (4n_0^2 m_p c^2)$ at an observer time $t_d = r_d / c = (2 \frac{E_{\text{iso}}}{m_p c^2})^{1/2}$, where a relation $dr = 2 \frac{E_{\text{iso}}}{m_p c^2} dt$ has been taken for superluminal motion. At the deceleration phase, the dynamics could be well described by the Blandford & McKee (1976) self-similar solution, where $r \propto t^{3/2}$ / $t^{3/8}$. (3) As the jet continues to decelerate, the Lorentz factor drops to $\Gamma = \Gamma_j$ at a time $t_j = t_d (\Gamma_0 / \Gamma_j)^{8/3}$, corresponding to a radius $r_j = r_d (\Gamma_0 / \Gamma_j)^{2/3}$. From the time on the transverse size of causally connected regions exceeds that of the jet, therefore the sphere approximation breaks down, and the jet starts expanding sideways. The dynamical evolution in this stage depends on the degree of sideways expansion. If the lateral velocity in the comoving frame equals to the local sound speed, the jet will spread quickly with the opening angle increasing and dropping exponentially (Rhoads 1999). At this stage, the radius hardly increases and may be regarded as a constant $r = r_j$, and $r \propto t^{1/2}$. (4) Finally the jet goes into NR phase with $\Gamma = 1$ at $t_{\text{NR}} = t_j = \frac{r_j}{c}$, where the evolution can be well described by Sedov-Taylor solution $r \propto t^{3/2}$ / $t^{3/5}$, with $\Gamma = (1 - \Gamma_j^2)^{1/2}$. In summary, the evolution is:

$$\begin{aligned} \text{coasting: } & t < t_d & \Gamma & = \Gamma_0; r \propto t \\ \text{sphere: } & t_d < t < t_j & \Gamma & \propto t^{-3/8}; r \propto t^{1/4} \\ \text{spreading: } & t_j < t < t_{\text{NR}} & \Gamma & \propto t^{-1/2}; r = r_j \\ \text{NR: } & t > t_{\text{NR}} & \Gamma & \propto t^{-3/5} (\Gamma_j); r \propto t^{2/5} \end{aligned} \quad (1)$$

Using the above simplified dynamical relation, the NR time and radius, defined as where $\Gamma = 1$, are able to be calculated as

$$t_{\text{NR}} = \frac{1}{2c} \frac{3E_j}{2m_p c^2 n}^{1/3}; \quad r_{\text{NR}} = r_j = \frac{3E_j}{2m_p c^2 n}^{1/3} \quad (2)$$

They are independent of Γ_0 and Γ_j . With typical values $E_j = 10^{51} E_{j,51}$ ergs and $n = 1 \text{ cm}^{-3}$ (e.g., Fraile et al. 2001; Panaitescu & Kumar 2001), we have

$$t_{\text{NR}} = 130 \frac{E_{j,51}^{1/3}}{n} \text{ d}; \quad (3)$$

Note that this t_{NR} refers to the PJ.

As for the RJ, it also transits into NR phase at a radius r_{NR} . However, due to the light travel time the observer time epoch is delayed by a time $2r_{\text{NR}}/c$, so the observed NR time for the RJ is

$$t_{\text{NR}}^{\text{RJ}} = t_{\text{NR}} + \frac{2r_{\text{NR}}}{c} = 5t_{\text{NR}}; \quad (4)$$

5 times that of the PJ².

There are uncertainties about the lateral spreading of jets, and it might be that little spreading occurs, as shown in some numerical simulations (e.g., Cannizzo et al. 2004). If we assume the extreme case that the lateral velocity is zero, then the jet remains conical geometry and continues to evolve as if it was a conical section of a spherical relativistic blast wave after $\Gamma < \Gamma_j$. In this case, the NR time for the PJ is $t_{\text{NR}} = (1/2) (3E_j / 2m_p c^2 n)^{1/3} =$

$610 (E_{j,51} / n_0^2)^{1/3} \text{ d}$, with $\Gamma_j = 10$, and the corresponding radius is $r_{\text{NR}} = 2ct_{\text{NR}}$, therefore for the RJ, the NR time is $t_{\text{NR}}^{\text{RJ}} = t_{\text{NR}} + 2r_{\text{NR}}/c = 5t_{\text{NR}} = 8.4 (E_{j,51} / n_0^2)^{1/3} \text{ yr}$. These may be regarded as upper limits, while the values in eqs. (2-4) for the fastest spreading cases as lower limits.

2.2. Non-relativistic phase emission

For the detailed discussion of afterglow emission in NR phase, the readers might refer to Frail, Waxman & Kumar (2000), Livio & Waxman (2000) and Waxman (2004), we here only give brief introduction.

Consider also the PJ emission first. After t_{NR} , the evolution is described by the spherical NR self-similar evolution, with the PJ radius given by $r = r_{\text{NR}} (t/t_{\text{NR}})^{2/5}$, and the swept-up particle number is $N_e \propto (4\pi/3) nr^3$. Simply assume that the shocked material forms a thin and uniform shell, with the width $\Delta r = r$ and the post-shock thermal energy density $U = E_j / (4\pi r^2)$. The electron and magnetic field energy densities are assumed to be constant fraction ϵ_e and ϵ_B , respectively, of the post-shock thermal energy density U . The electrons are believed to be accelerated to form a power law distribution, $dn_e = dN_e / N_e^p$ for $N_e > N_m$. Based on the above assumptions, it can be found that the magnetic field strength and the minimum electron Lorentz factor evolve as $B \propto t^{-3/5}$ and $N_m \propto t^{-6/5}$, respectively.

The accelerated electrons will give rise to synchrotron emission. The characteristic synchrotron frequency of electrons with N_m is $\nu_m = eB^2 / (2m_e c)$, i.e.,

$$\nu_m = 0.3 \frac{e^2}{m_e} \frac{1}{B} \frac{1}{N_m} \frac{t}{t_{\text{NR}}} \text{ GHz}; \quad (5)$$

where $\epsilon_e = 10^{-1}$, and $\epsilon_B = 10^{-1}$. The peak specific luminosity is $L_m = N_e P_m$ where $P = (4\pi/3) T_c^2 (B^2/8)$ is the synchrotron power of an electron with N_m . The observed radio frequency is usually beyond ν_m at NR stage, the specific luminosity is therefore $L = L_m (\nu / \nu_m)^{(1-p)/2} / t^{2(1-p)/2} = 3p/2$, and given by

$$L = 4 \frac{10^{30}}{10 \text{ GHz}} \frac{e^2}{m_e} \frac{1}{B} \frac{1}{N_m} \frac{t}{t_{\text{NR}}} \text{ ergs s}^{-1} \text{ Hz}^{-1}; \quad (6)$$

where $p = 2$ has been taken. The NR light curve attens, compared with the decay, $\propto t^{-p}$, in the spreading phase (Rhoads 1999; Sari, Piran & Halpern 1999).

As for the RJ, when it is still relativistic the emission is always beamed away from us and hence invisible. At the time $t_{\text{NR}}^{\text{RJ}}$ after the GRB, the RJ becomes non-relativistic and the emission becomes isotropic. The observed RJ luminosity at this point should be comparable to that of the PJ at t_{NR} , because of the same characteristics of the PJ and RJ. If neglect the NR jet velocity with respect to the light speed, the time delay between the emission from the PJ and RJ could be roughly fixed as $2r/c = 2r_{\text{NR}}/c = 4t_{\text{NR}}$ (for r is not r_{NR}). The RJ specific luminosity, then, could be written as, for $t > t_{\text{NR}}^{\text{RJ}}$,

$$L^{\text{RJ}}(t) \approx L(t = 4t_{\text{NR}}) / \frac{t}{t_{\text{NR}}} \frac{4t_{\text{NR}}}{t_{\text{NR}}} \quad (7)$$

² It can be shown that the factor 5 is also valid for the wind case where the external density decreases as the square of the distance from the source (Dai & Lu 1998; Chevalier & Li 2000).

A schematic plot is given in figure 1 for both PJ and RJ radio light curves. After rapid increase in flux, the RJ emission reaches the peak at around t_{NR}^{RJ} , and then decreases as a delayed light curve of the NR-phase PJ, but showing a steeper decline in the logarithmic plot. Note that the transition to NR phase might be gradual, and the jet edge might be not sharp, therefore both these can smooth the RRB feature on the plot.

3. observation

3.1. GRB 970508 and GRB 980703

As discussed above, if a GRB can be monitored for a long time in radio bands, e.g., a few years, the RRB may be able to be detected. So far, there are two GRBs that have been reported in the literatures with radio monitoring longer than one year: GRB 970508 and GRB 980703 (Frail, Waxman & Kulkarni 2000; Berger, Kulkarni & Frail 2001; Frail et al. 2003).

Frail, Waxman & Kulkarni (2000) report an extensive monitoring of the radio afterglow of GRB 970508, lasting 450 days after the burst. In the data analysis they found that the spectral and temporal radio behavior indicate a transition to NR expansion at $t_{NR} = 100$ d, therefore, we should expect the RRB at around day 500. However, this is unfortunately behind the last observation of this burst, so we might have missed that apparent phenomena.

GRB 980703 was monitored even longer, up to 10^3 d, as shown in figure 1 of Frail et al. (2003). Two obvious attenuations appear in the radio light curves: while the late-time transition to a constant flux is thought to be the host galaxy contribution, the earlier attenuation at 40 d is attributed to the transition into NR expansion (Berger, Kulkarni & Frail 2001). Modelling the evolution has also inferred a similar value of $t_{NR} = 30 - 50$ d (Frail et al. 2003). Therefore, the expected RRB should arise at

200 d, and then after another time interval of 200 d, around 400 d from the burst, the radio flux should decline to a value similar to just before the RRB. At first glance of figure 1 of Frail et al. (2003), the radio light curves, somewhat more extensive at 8.5 and 4.8 GHz, seem to show only decays without any re-brightening. However, we notice that there is no observation data collected between 210 d and 400 d, therefore the RRB may be missed once again due to the lack of observation.

3.2. Prediction for GRB 030329

GRB 030329 is the nearest cosmological burst ($z = 0.1685$), and has a bright afterglow at all wavelengths. Berger et al. (2003) have reported its bright radio afterglow up to 70 d after the burst. Since no radio attenuation (due to transition to NR evolution) appears yet³, we should calculate t_{NR} using $E_{j;51=n}$ derived from available data.

The early breaks (< 0.5 d) in the R band (Price et al. 2003) and X-ray (Tiengo et al. 2004) light curves infer a small jet opening angle, leading to a small jet-corrected energy release in GRB 030329, which is more than one order of magnitude below the average value around which most

GRBs are narrowly clustered (Frail et al. 2001; Panaitescu & Kumar 2001). Two models have been proposed to solve this problem: a refreshed-shock model with 10 times more energy injected later (Granot, Nakar & Piran 2003); and a two-component model with most energy in a wider jet component (Berger et al. 2003). Both models have the same result: the kinetic energy corresponding to the late-time radio afterglow is typical for all GRBs. Based mainly on the early multi-frequency data, a typical value for medium density, $n = 1 \text{ cm}^{-3}$, was also derived by Willingale et al. (2004). Therefore, the estimated value of t_{NR} should be typical as in eq. (3), hence $t_{NR} = 130$ d. In fact, the radio angular size measurement of this burst shows relativistic expansion 83 d after the burst (Taylor et al. 2004), consistent with the estimation here.

In addition, Berger et al. (2003) have inferred $E_{j;51=n} = 0.14 \frac{1=2}{c;13} \text{ erg}$ from a snapshot spectrum at $t_j = 10$ d, where $c = c = 10^{13} \text{ Hz}$ is the cooling frequency. This parameter value leads to a too early NR phase, $t_{NR} = 68$ d (from eq. 3), connected with the observed superluminal expansion (Taylor et al. 2004). However, in the parameter derivation, the assumption of jet break time at $t_j = 10$ d might be incorrect, because the millimeter observation shows that the light curves have already steepened at 5 d at both 100 and 250 GHz (Sheth et al. 2003), implying that $t_j < 5$ d. Moreover, the angular size evolution can also give constraints to the model parameters. For GRB 030329, Granot, Ramirez-Ruiz & Loeb (2004) derive $E_{j;51=n} = 0.8$ (see also Oren, Nakar & Piran 2004) from the observation by Taylor et al. (2004). This yields a later transition at $t_{NR} = 120$ d.

We will take the more reasonable value $t_{NR} = 120$ d (It should be noticed that this might still be the lower limit since the most rapid sideways spreading has been assumed), and hence the expected RRB should arise at 1.7 yr after GRB 030329, with the fluxes comparable to that at the time t_{NR} . Assuming the same temporal slope for late time, an extrapolation of the available radio light curves (Berger et al. 2003) to 120 d gives a flux 0.6 mJy at 15 GHz, or 0.3 mJy at 44 GHz. Dense monitoring campaign around 1.7 yr after GRB 030329 is required to obtain a well-observed RRB profile.

4. summary and discussion

In this work we suggest that RRBs are common for GRBs with double-sided jets, which come from the RJ transition to NR evolution. If we assume the same properties for both PJ and RJ and also for the ambient medium on both sides, the RRB would arise at a time $t_{NR}^{RJ} = 5t_{NR} = 1.8 (E_{j;51=n})^{1=3} \text{ yr}$ after the burst, with a flux comparable to that at the time t_{NR} . After t_{NR}^{RJ} , the afterglow behaves as a delayed emission of that behind t_{NR} , with the time lag of $4t_{NR}$ (eq. 7). Unfortunately, no radio data could be collected when RRBs occur for GRB 970508 and GRB 980703, two longest observed GRBs so far. We suppose the RRB of GRB 030329 around 1.7 yr after the burst with 0.6 (0.3) mJy at 15 (44) GHz, and urge dense

³ Although the X-ray afterglow shows an attenuation around day 37 (Tiengo et al. 2004), we believe this is not relevant to the relativistic to NR transition of the radio jet, because of no simultaneous radio attenuation (Berger et al. 2003), and also connected with the still superluminal expansion in the radio angular size measurement (Taylor et al. 2004). The X-ray attenuation may need other explanations, e.g. an IC component; NR transition for the narrow jet in two-component model (Berger et al. 2003).

monitoring campaign during that time. It should be noticed that for weak jet-spreading, the RRB might be more delayed since t_{NR}^R is much larger (see in the end of x2.1).

There has been growing evidence for collimated jets in GRBs over the past several years, which is coming mainly from observations of achromatic breaks in the afterglow light curves (e.g., Kulkarni et al. 1999; Stanek et al. 1999). However, there are still other explanations for the light curve breaks, for example, the transition from the relativistic to NR phase of the blast wave at a few days due to highly dense medium (Dai & Lu 1999; Wang, Dai & Lu 2000); the effects of IC scattering attenuating or steepening the light curves (Wei & Lu 2000); a sudden drop in the external density (Kumar & Panaitescu 2000); a break in the energy spectrum of radiating electrons (Li & Chevalier

2001). On the other hand, though black hole-disk system with twin jets is generally assumed in GRBs, magnetized, rapidly rotating neutron stars remain contenders, and an off-center dipole could lead to a one-sided jet. Since RRBs are only associated with collimated, double-sided, relativistic outflows, the detection of RRBs would provide straightforward evidence of double-sided jets in GRBs, and prove the black hole-disk system formation in the cores of progenitors. This makes RRB observations significantly important.

Z. Li thanks R. F. Shen for discussions, and L. J. Gou for comments. This work was supported by the National 973 Project and the Special Funds for Major State Basic Research Projects.

REFERENCES

- Berger, E., et al. 2003, *Nature*, 426, 154
 Berger, E., Kulkarni, S. R., & Frail, D. A. 2001, *ApJ*, 560, 652
 Cannizzo, J. K., Gehrels, N., & Vishniac, E. T. 2004, *ApJ*, 601, 380
 Chevalier, R. A., & Li, Z.-Y. 2000, *ApJ*, 536, 195
 Dai, Z. G. & Gou, L. J. 2001, *ApJ*, 552, 72
 Dai, Z. G. & Lu, T. 1998, *MNRAS*, 298, 87
 Dai, Z. G. & Lu, T. 1999, *ApJ*, 519, L155
 Dalal, N., Griest, K., & Puet, J. 2002, *ApJ*, 564, 209
 Frail, D. A., et al. 2001, *ApJ*, 562, L55
 Frail, D. A., et al. 2003, *ApJ*, 590, 992
 Frail, D. A., Waxman, E., & Kulkarni, S. R. 2000, *ApJ*, 537, 191
 Granot, J. & Kumar, P. 2003, *ApJ*, 591, 1086
 Granot, J. & Loeb, A. 2003, *ApJ*, 593, L81
 Granot, J., Nakar, E., & Piran, T. 2003, *Nature*, 426, 138
 Granot, J., Panaitescu, A., Kumar, P., & Woosley, S. E. 2002, *ApJ*, 570, L61
 Granot, J., Ramirez-Ruiz, E., & Loeb, A. 2004, (astro-ph/0407182)
 Hjorth, J., et al. 2003, *Nature*, 423, 847
 Kulkarni, S. R., et al. 1999, *Nature*, 398, 389
 Kumar, P. & Panaitescu, A. 2000, *ApJ*, 541, L51
 Li, Z.-Y. & Chevalier, R. A. 2001, *ApJ*, 551, 940
 Livio, M. & Waxman, E. 2000, *ApJ*, 538, 187
 Meszaros, P. 2002, *ARA & A*, 40, 137
 Meszaros, P., Rees, M. J., & Wijers, R. A. M. J. 1998, *ApJ*, 499, 301
 Oren, Y., Nakar, E., & Piran, T. 2004, preprint (astro-ph/0406277)
 Panaitescu, A. & Kumar, P. 2001, *ApJ*, 560, L49
 Panaitescu, A. & Kumar, P. 2002, *ApJ*, 571, 779
 Piran, T. 2004, *Rev. Mod. Phys.*, accepted (astro-ph/0405503)
 Price, P. A., et al. 2003, *Nature*, 423, 844
 Rhoads, J. E. 1997, *ApJ*, 487, L1
 Rhoads, J. E. 1999, *ApJ*, 525, 737
 Rossi, E., Lazzati, D., & Rees, M. J. 2002, *MNRAS*, 332, 945
 Sari, R., Piran, T., & Halpern, J. P. 1999, *ApJ*, 519, L17
 Sheth, K., Frail, D. A., White, S., Das, M., Bertoldi, F., Walter, F., Kulkarni, S. R., & Berger, E. 2003, *ApJ*, 595, L33
 Stanek, K. Z., Gammavich, P. M., Kaluzny, J., Pynch, W., & Thompson, I. 1999, *ApJ*, 522, L39
 Taylor, G. B., Frail, D. A., Berger, E., & Kulkarni, S. R. 2004, *ApJ*, 609, L1
 Tiengo, A., Mereghetti, S., Ghisellini, G., Tavecchio, F., & Ghirlanda, G. 2004, *A & A*, 423, 861
 Wang, X. Y., Dai, Z. G., & Lu, T. 2000, *MNRAS*, 317, 170
 Waxman, E. 2004, *ApJ*, 602, 886
 Wei, D. M. & Lu, T. 2000, *A & A*, 360, L13
 Willingale, R., Osborne, J. P., O'Brien, P. T., Ward, M. J., Levan, A., & Page, K. L. 2004, *MNRAS*, 349, 31
 Zhang, B. & Meszaros, P. 2002, *ApJ*, 571, 876
 Zhang, B. & Meszaros, P. 2004, *Int. J. Mod. Phys. A*, 19, 2385

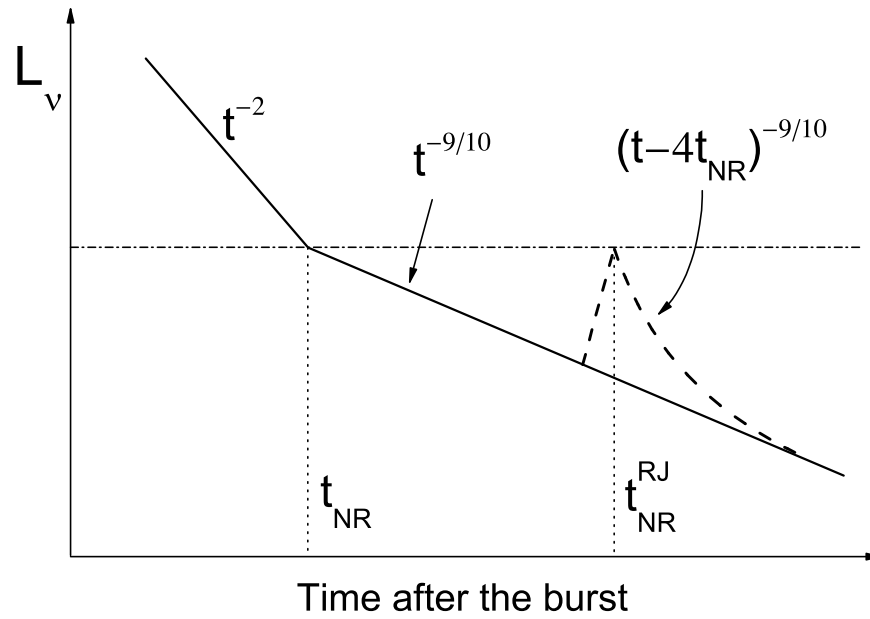


Fig. 1. The schematic log-log plot for the radio light curve at $\nu > \nu_m$. The solid and dashed lines correspond to the contribution from the P J and R J, respectively. The time scalings are marked, assuming $p = 2$. After a steep decline in the spreading phase, the P J light curve attenuates at t_{NR} . The R J emission rapidly increases to a peak around $t_{NR}^{RJ} = 5t_{NR}$, and then declines following the way of the P J unless a time delay of $4t_{NR}$, but exhibiting steep light curve in the log-log plot. The dashed-dot line indicates $L(t_{NR}) = L^{RJ}(t_{NR}^{RJ})$.